Available online at www.sciencedirect.com
ScienceDirect
Chinese Journal of Natural Medicines 2022, **20**(4): 301-308
doi: 10.1016/S1875-5364(21)60120-6
Chinese Journal of Natural Medicines

•Research article•

Polyhydroxylated eudesmane sesquiterpenoids and sesquiterpenoid glucoside from the flower buds of *Tussilago farfara*

LI Yu-Peng[1], YANG Kang[2], MENG Hui[2], SHEN Tao[2], ZHANG Hua[1*]

[1] *School of Biological Science and Technology, University of Jinan, Jinan 250022, China;*
[2] *Key Laboratory of Chemical Biology (MOE), School of Pharmaceutical Sciences, Shandong University, Jinan 250012, China*

Available online 20 Apr., 2022

[ABSTRACT] Chemical fractionation of the *n*-BuOH partition, which was generated from the EtOH extract of the flower buds of *Tussilago farfara*, afforded a series of polar constituents including four new sesquiterpenoids (**1**–**4**), one new sesquiterpenoid glucoside (**5**) and one known analogue (**6**) of the eudesmane type, as well as five known quinic acid derivatives (**7**–**11**). Structures of the new compounds were unambiguously characterized by detailed spectroscopic analyses, with their absolute configurations being established by *X*-ray crystallography, electronic circular dichroism (ECD) calculation and induced ECD experiments. The inhibitory effect of all the isolates against LPS-induced NO production in murine RAW264.7 macrophages was evaluated, with isochlorogenic acid A (**7**) showing significant inhibitory activity.

[KEY WORDS] *Tussilago farfara*; Eudesmane sesquiterpenoid; Anti-inflammation; NO production inhibition; Quinic acid derivative
[CLC Number] R284 **[Document code]** A **[Article ID]** 2095-6975(2022)04-0301-08

Introduction

Tussilago farfara (trivial name: coltsfoot) is a herbaceous plant and the only species of genus *Tussilago* L. (family Compositae) that occurs in most temperate regions of the world [1]. In addition to serving as an ornamental honey plant that is widely cultivated in many gardens [1], *T. farfara* has been well known as a medicinal species and used in traditional Chinese medicine since 2000 years ago [2]. Its dried flower buds, known as "Farfarae Flos" in Latin and "Kuandonghua" in Chinese, are collected by all editions of Chinese Pharmacopoeia under the entry of commonly used herbs and have been mainly applied in the treatment of respiratory disorders such as cough and asthma [2, 3]. In a very recent review, Liu *et al.* presented a comprehensive summary on the traditional uses, phytochemical and pharmacological studies of *T. farfara*, and the major constituents were shown to be terpenoids, organic acids, flavonoids, steroids and chromones [2]. Among these molecules, sesquiterpenoids especially of the bisabolane and oplopane types are the characteristic constituents of *T. farfara* and have also been mostly investigated [2].

As part of our continuing efforts to pursue small molecule natural products with interesting bioactivities [4-8], the previous studies on the EtOAc partition from the ethanolic extract of *T. farfara* have yielded an array of diverse isolates including chromane enantiomers [9], indole alkaloids [10] and sesquiterpenoids [11]. As many respiratory diseases are closely related with inflammatory responses, these isolates have been primarily screened in an *in vitro* inhibitory assay against NO (nitric oxide) release in murine RAW264.7 cells, but none of them showed obvious activities. Considering the fact that most traditional medications containing *T. farfara* are in the form of decoction from water boiling, we have guessed that the active ingredients equivalent to the traditional medicinal effect of this herb might exist in the polar fractions. Therefore, the chemical constituents in the *n*-BuOH partition were further intensively investigated. As a result, six eudesmane-type sesquiterpenoids (**1**−**6**) including a glucoside (**5**) (Fig. 1), as well as five chlorogenic acid analogues (**7**−**11**) (Fig. S1, Supporting Information), were obtained and identified, with compounds **1**−**5** being described for the first time. The *α*-glucosidase and NO production inhibitory activities of all the isolates were assessed, while only the known isochlorogenic acid A (**7**) showed inhibition against NO release. Details of the isolation, structure characterization and bioactivity testing of these compounds are described below.

Results and Discussion

Compound **1** was assigned the molecular formula of

[Received on] 21-Nov.-2021
[Research funding] This work was supported by the Natural Science Foundation of Shandong Province (No. JQ201721), the Young Taishan Scholars Program (No. tsqn20161037) and Innovation Team Project of Jinan Science & Technology Bureau (No. 2018GXRC003).
[*Corresponding author] Tel: 86-531-89736199, E-mail: bio_zhangh@ujn.edu.cn
These authors have no conflict of interest to declare.

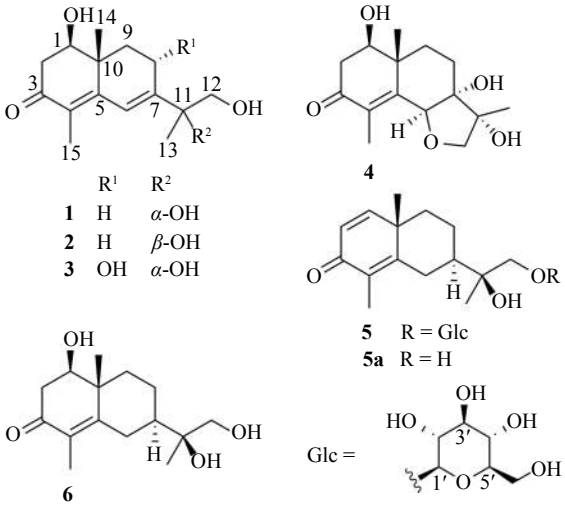

Fig. 1 Chemical structures of 1–6

$C_{15}H_{22}O_4$ by (+)-HR-ESIMS analysis at *m/z* 267.1593 ([M + H]$^+$, Calcd. 267.1591), indicating five degrees of unsaturation. The ^{1}H NMR data (Table 1) of **1** revealed characteristic resonances for an olefinic [δ_H 6.81 (dd, J = 2.4, 0.9 Hz)], an oxygenated methine [δ_H 3.73 (dd, J = 12.5, 5.7 Hz)], an oxymethylene [δ_H 3.60 and 3.52 (both d, J = 11.1 Hz)] and three tertiary methyl [δ_H 1.84, 1.32, 1.05] protons, while the ^{13}C NMR data (Table 2) showed 15 signals corresponding to a conjugated ketone (δ_C 200.3), four olefinic (δ_C 120.5, 128.7, 156.2, 157.6), two sp^3 quaternary [δ_C 76.8 (*O*-bonded), 39.8], an oxygenated methine (δ_C 74.0), four methylene [δ_C 69.8 (*O*-bonded), 43.2, 39.8, 33.6] and three methyl (δ_C 23.8, 15.3, 10.4) carbons. These observations accounted for three degrees of unsaturation and the remaining two required a bicyclic scaffold for **1**. Analysis of ^{1}H–^{1}H COSY data (Fig. 2) afforded two proton-bearing fragments (CH-1 to CH_2-2 and CH_2-8 to CH_2-9) which were further connected by the HMBC correlations from H_3-14 to C-1, C-5, C-9 and C-10 (Fig. 2). Other key HMBC correlations included those from H_2-2 to C-3, H_3-15 to C-3, C-4 and C-5, and H-6 to C-5, C-7 and C-8, which returned the bicyclic skeleton of **1** as shown. Finally, the HMBC signals from H_3-13 to C-7, C-11 and C-12 confirmed the location of the oxygenated isopropyl side chain (C-11 to C-13) at C-7. The presence of 1-OH, 11-OH and 12-OH was indicated by the molecular constitution and the chemical shifts for C-1 (δ_C 74.0), C-11 (δ_C 76.8) and C-12 (δ_C 69.8). The planar structure of **1** was thus established to possess a eudesmane sesquiterpenoid skeleton as drawn (Fig. 2).

The relative configuration of **1** was determined by analysis of the NOESY spectrum (Fig. 3). The correlations of H_3-14 with H-2 at δ_H 2.65 and H-8 at δ_H 2.34 indicated that the two protons and Me-14 were all axially bonded (1,3-diaxial relationship) in the two six-membered rings, and they were assigned to be *β*-orientated. Thus H-9 at δ_H 2.16 also took a *β*-orientation based on its NOESY correlation with H_3-14 and coupling patterns with H_2-8 (J = 4.8, 2.2 Hz), while the strong NOESY correlation of H-1 with H-9*α* (δ_H 1.38) supported the *α*- and *β*-orientations for H-1 and 1-OH, respectively. Owing to the rotary nature of the C-11 to C-13 side chain around C-7–C-11 single bond, special cautions should be taken when determining the configuration at C-11, and a 11R^* relative configuration was tentatively assigned by careful conformational analyses as well as the NOESY correlations of H_3-13 with both H-8α and H-8*β* (Fig. 3). Finally, the structure of **1** was corroborated by single-crystal X-ray crystallography with Cu-K*α* radiation (*λ* = 1.54184 Å) [Flack

Table 1 ^{1}H NMR data for compounds 1–4 (600 MHz, δ in ppm and *J* in Hz)

No.	1[a]	2[a]	3[a]	4[a]	4[b]
1	3.73, dd (12.5, 5.7)	3.73, dd (12.5, 5.7)	3.79, dd (12.7, 5.5)	3.75, dd (12.8, 5.6)	4.18, dd (12.8, 5.4)
2*α*	2.58, dd (17.2, 5.7)	2.58, dd (17.2, 5.7)	2.56, dd (17.2, 5.5)	2.58, dd (17.1, 5.6)	3.02, dd (16.8, 5.4)
2*β*	2.65, dd (17.2, 12.5)	2.65, dd (17.2, 12.5)	2.64, dd (17.2, 12.7)	2.65, dd (17.1, 12.8)	3.10, dd (16.8, 12.8)
6	6.81, dd (2.4, 0.9)	6.81, t (1.6)	6.77, d (1.8)	4.87[c]	5.45, d (1.5)
8*α*	2.39, m	2.37, m (2H)		1.62[d]	1.91, m
8*β*	2.34, m		4.67, ddd (10.5, 5.6, 1.8)	1.78, ddd (14.0, 13.3, 3.4)	1.98, m
9*α*	1.38, ddd (13.1, 11.5, 6.1)	1.36, m	1.41, dd (12.6, 10.5)	1.64[d]	2.23, ddd (13.7, 13.2, 3.7)
9*β*	2.16, ddd (13.1, 4.8, 2.2)	2.18, m	2.47, dd (12.6, 5.6)	1.95, m	2.45, dt (13.2, 3.6)
12	3.60, d (11.1)	3.62, d (11.1)	3.63, d (10.9)	*α* 3.84, d (9.6)	*α* 4.33, d (9.3)
	3.52, d (11.1)	3.51, d (11.1)	3.72, d (10.9)	*β* 3.97, d (9.6)	*β* 4.19, d (9.3)
13	1.32, s	1.32, s	1.47, s	1.23, s	1.48, s
14	1.05, s	1.05, s	1.09, s	1.19, s	1.62, s
15	1.84, s	1.84, s	1.84, s	1.85, s	2.00, s

[a] Measured in methanol-d_4; [b] Measured in pyridine-d_5; [c] Signals overlapped by solvent peak; [d] Overlapping signals within the same column

Table 2 ^{13}C NMR data for compounds **1**–**5** and **5a** (150 MHz, δ in ppm)

No.	**1**[a]	**2**[a]	**3**[a]	**4**[a]	**4**[b]	**5**[a,d]	**5a**[a]	**5a**[c]
1	74.0	74.0	73.4	74.6	74.2	159.9	160.0	157.4
2	43.2	43.2	42.7	43.4	44.3	126.4	126.4	125.3
3	200.3	200.3	200.1	200.3	198.8	188.6	188.6	185.1
4	128.7	128.5	130.2	137.7	136.8	130.0	129.8	127.6
5	157.6	157.7	156.3	157.1	156.8	164.4	164.6	161.7
6	120.5	120.2	123.1	78.7	79.0	29.9	29.8	28.3
7	156.2	156.7	155.2	80.2	80.3	48.1	47.4	45.8
8	23.6	23.6	67.0	26.0	26.4	22.2	22.1	20.6
9	33.6	33.9	43.9	32.4	32.9	39.1	39.1	37.8
10	39.8	39.9	42.3	41.2	41.4	42.1	42.1	40.2
11	76.8	76.9	77.8	80.0	79.6	74.6	74.9	72.8
12	69.8	69.4	71.0	78.5	78.7	76.7	68.9	67.7
13	23.8	24.3	24.5	18.0	19.0	22.0	22.1	22.3
14	15.3	15.3	16.3	17.8	18.6	23.6	23.6	22.9
15	10.4	10.4	10.6	10.7	11.3	10.6	10.5	10.1

[a] Measured in methanol-d_4; [b] Measured in pyridine-d_5; [c] Measured in DMSO-d_6; [d] Data for sugar moiety: δ_C 105.0 (C-1′), 75.2 (C-2′), 78.0 (C-3′), 78.1 (C-4′), 71.7 (C-5′), 62.8 (C-6′)

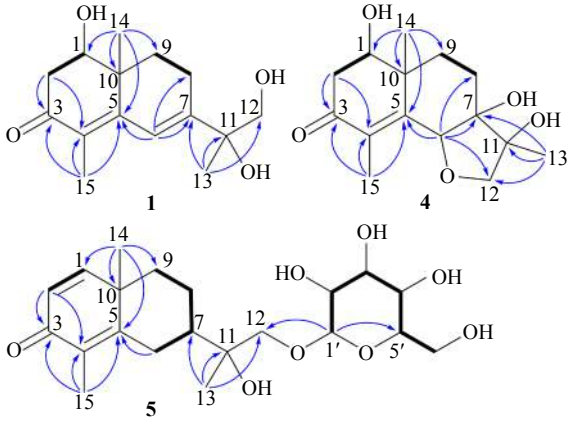

Fig. 2 ^{1}H–^{1}H COSY (bond lines) and key HMBC (arrows) correlations for **1**, **4** and **5**

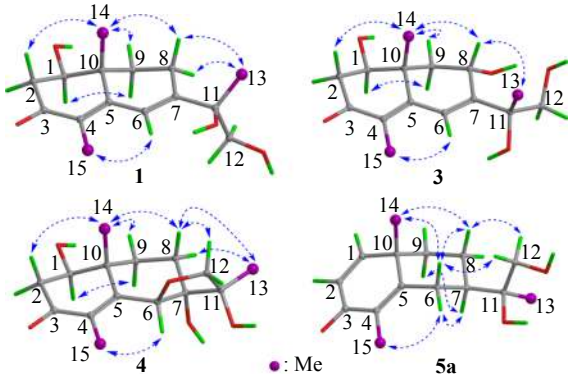

Fig. 3 Key NOESY correlations (two headed dashed arrows) for **1**, **3**, **4** and **5a**

parameter 0.19 (12)] (Fig. 4), with the assigned absolute configuration being also consistent with that established by comparison between the experimental and calculated ECD spectra (Fig. 5). Moreover, the absolute configuration at C-11 was further confirmed by an *in situ* dimolybdenum-induced ECD experiment developed by Snatzke and Frelek [12], with a negative Cotton effect at 305 nm in the induced ECD spectrum (Fig. S2, Supporting Information). Compound **1** was thus unambiguously characterized.

Compound **2** possessed the same molecular formula ($C_{15}H_{22}O_4$) as **1** based on (+)-HR-ESIMS analysis at *m*/*z* 267.1593 ([M + H]$^+$, Calcd. 267.1591), suggestive of an isomer of the latter. The ^{1}H and ^{13}C NMR data (Tables 1 and 2) of **2** were highly similar to those of **1**, with only the chemicals shifts for C-7, C-9, C-12 and C-13 (≥ 0.3 ppm) varying obviously. Examination of 2D ^{1}H–^{1}H COSY and HMBC NMR data (Figs. S13 and S15, Supporting Information) returned an identical constitution structure with **1**, and further analysis of NOESY spectrum (Fig. S16, Supporting Information) suggested that the relative configurations of their bicyclic cores were also the same. However, unlike compound **1** whose H_3-13 showed remarkable NOESY correlations with both H-8*α* and H-8*β*, such correlations were not observed for **2**, implying that the two co-metabolites should be C-11 epimers. As shown in Fig. 5, the ECD spectra of **1** and **2** were very similar with consistent curve trend, supporting that they had identical absolute configuration for the bicyclic frame-

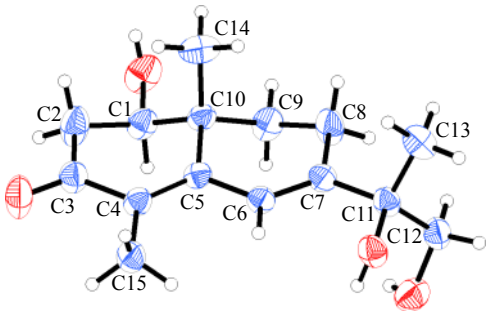

Fig. 4 X-ray crystallographic structure for 1

work. The C-11 configuration of **2** was eventually established to be *S* also *via* the dimolybdenum-induced ECD experiment, with a positive Cotton effect at 315 nm (Fig. S2, Supporting Information).

Compound **3** was assigned the molecular formula of $C_{15}H_{22}O_5$ by (+)-HR-ESIMS analysis at *m/z* 283.1538 ([M + H]$^+$, Calcd. 283.1540), with 16 mass units more than that of **1** indicative of an oxygenated analogue. Analysis of the ^{1}H and ^{13}C NMR data (Tables 1 and 2) for **3** confirmed this hypothesis, with diagnostic signals for an oxymethine (δ_H 4.67, δ_C 67.0, CH-8) in **3** replacing those for a methylene (δ_H 2.39 and 2.34, δ_C 23.6, CH_2-8) in **1**. Further inspection of 2D ^{1}H–^{1}H COSY and HMBC NMR data (Figs. S20 and S22, Supporting Information) revealed key correlations of H_2-9/H-8 and H-8/C-6 & C-7, which located the new hydroxy group at C-8. Furthermore, the NOESY data (Fig. 3) showed NOE interactions of H_3-14 with H-2β, H-8 and H-9β, as well as H-1α with H-9α, suggesting that the relative configurations at C-1 and C-10 in **3** were identical with those in **1** and 8-OH was α-directed. The absolute configuration of the bicyclic core of **3** was established as shown on the basis of its similar ECD curve with that of **1** (Fig. 5), while the C-11 configuration was assigned to be *R* (same as **1**) based on the negative Cotton effect at 304 nm in the induced ECD spectrum (Fig. S2, Supporting Information).

Compound **4** possessed the same molecular formula ($C_{15}H_{22}O_5$) as **3** based on (+)-HR-ESIMS analysis at *m/z* 283.1537 ([M + H]$^+$, Calcd. 283.1540), being isomeric with the latter and bearing five degrees of unsaturation. Analysis of the NMR data (Tables 1 and 2) for **4** revealed the presence of an α, β-unsaturated ketone group (δ_C 200.3, 157.1, 137.7) occupying two degrees of unsaturation, and the remaining three suggested a tricyclic skeleton for **4**. Further examination of 2D ^{1}H–^{1}H COSY and HMBC NMR data (Fig. 2) returned identical spin coupling systems with those (CH-1 to CH_2-2 and CH_2-8 to CH_2-9) in **1**, as well as crucial HMBC correlations from H_2-2 to C-3, H-6 to C-5, C-7 and C-8, H_3-14 to C-1, C-5, C-9 and C-10, and H_3-15 to C-3, C-4 and C-5. In addition, the chemical shift for C-6 (δ_C 78.7) and the key HMBC signal from H-6 to C-12 (δ_C 78.5) indicated the connection between C-6 and C-12 *via* an ether bond. Considering the molecular constitution and the chemical shift (δ_C 80.2) for C-7, an extra hydroxy group at C-7 was also assigned. The planar structure of **4** was hence established as

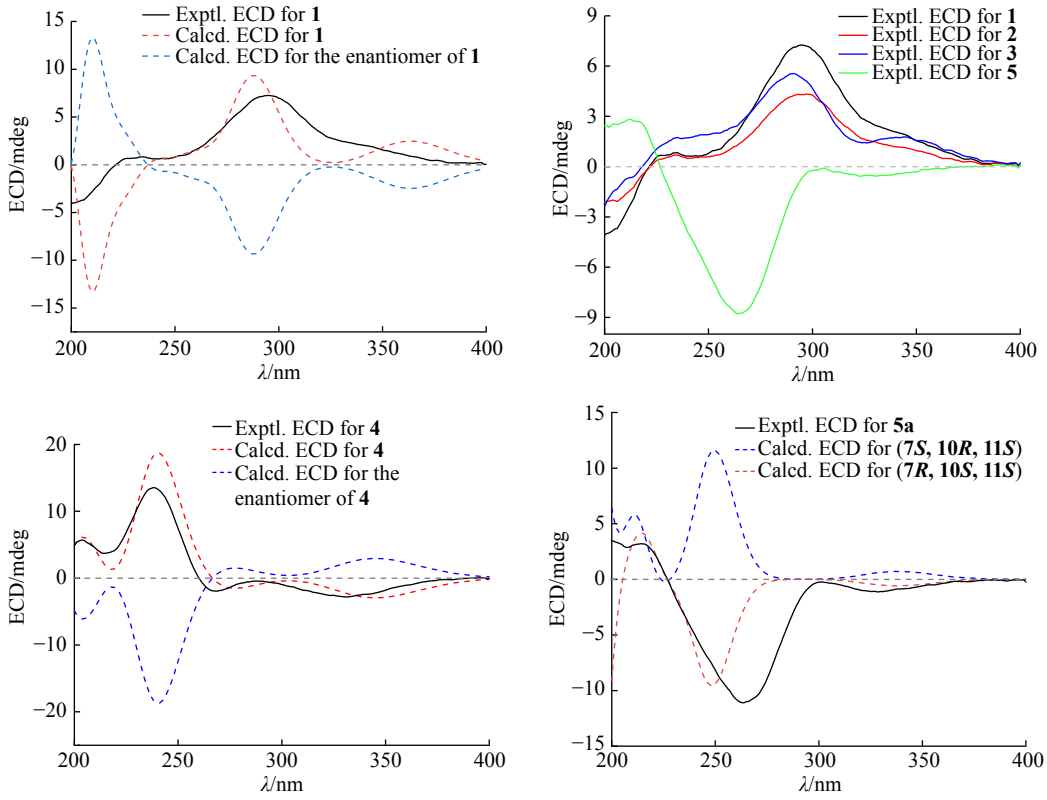

Fig. 5 Experimental ECD spectra for 1–5 and 5a compared with the calculated ECD spectra for 1, 4 and 5a

drawn (Fig. 2).

The relative configuration of **4** was determined by analysis of NOESY data (Fig. 3) as described below. Similar to **1**, Me-14 and 1-OH in **4** were assigned to be *β*-directed by the NOESY correlation of H-1 with H-9*α* and those of H_3-14 with H-2*β*, H-8*β* and H-9*β*. Then the cross-peak between H-8*β* and H-12 at δ_H 3.97 suggested the close steric relationship for CH_2-8 and CH_2-12 groups, which required ring-B and ring C to possess a *cis*-conjunction and thus H-6 and 7-OH was both *α*-positioned. Lastly, H_3-13 showed strong NOESY correlations with both H-8*α* and H-8*β*, indicating a *β*-orientation for Me-13 as in **1**. The absolute configuration of **4** was finally determined by comparing its experimental ECD curve with the computed ones for the two possible isomers (Fig. 5), which revealed an excellent match with the (1*R*, 6*S*, 7*S*, 10*R*, 11*R*)-enantiomer.

Compound **5** was assigned the molecular formula of $C_{21}H_{32}O_8$ by (+)-HR-ESIMS analysis at *m*/*z* 413.2165 ([M + H]$^+$, calcd 413.2170). The ^{1}H NMR data (Table 3) of **5** showed a diagnostic signal at δ_H 4.30 (d, *J* = 7.8 Hz) for the anomeric proton of a sugar moiety, which along with the carbon resonances (Table 2) at δ_C 105.0, 78.1, 78.0, 75.2, 71.7 and 62.8 suggested the presence of a *β*-glucopyranoside. Apart from the sugar unit, the NMR data for **5** also displayed typical signals for a conjugated carbonyl (δ_C 188.6) and four olefinic carbons (δ_C 164.4, 159.9, 130.0, 126.4), as well as three tertiary methyl groups (δ_H 1.91, 1.27, 1.26; δ_C 23.6, 22.0, 10.6). Further analysis of ^{1}H–^{1}H COSY data (Fig. 2) constructed two structural fragments, *i.e.* Δ^1 and CH_2-6 to CH_2-9, which together with the key HMBC correlations from H-2 to C-3, H_2-6 to C-5, H_3-14 to C-1, C-5, C-9 and C-10, H_3-13 to C-7, C-11 and C-12, and H_3-15 to C-3, C-4 and C-5, constructed the planar structure of the aglycone moiety as shown, incorporating a dienone functionality. Lastly, the sugar unit was attached to C-12 by the HMBC correlation from H-1′ to C-12 to finalize the constitution structure of **5** as shown.

Subsequent enzymatic hydrolysis of **5** with snailase afforded the free aglycone (**5a**) and sugar, the latter being determined to be d-glucose by comparing the HPLC chromatograms of the acetylated derivative with those from the standard $_D$- and $_L$-glucoses (Fig. S41, Supporting Information). The relative configuration of the bicyclic core of **5a** was established by analysis of NOESY data and ^{1}H–^{1}H couplings (in DMSO-d_6, Fig. 3 and Table 3). The correlations of H_3-14 with both H-6 at δ_H 2.05 and H-8 at δ_H 1.62 implied that the right-side ring took a chair form conformation and Me-14 and the two protons were all axially bonded (1, 3-diaxial relationship), and they were randomly assigned to be *β*-orientated. Then H-7 was also established to be axially bonded and thereby α-directed on the basis of the magnitude of $J_{6\beta,7}$ (12.8 Hz, 1,2-diaxial relationship). The absolute configuration assignment for **5a** first started from C-11 that was determined to be *S*-configured based on the positive Cotton effect at 312 nm in the induced ECD spectrum (Fig. S2, Supporting Information), while the bicyclic moiety was assigned a (7*R*, 10*S*)-configuration by comparing the measured ECD spectrum with the calculated ones (Fig. 5). The structure with absolute configuration of **5** was hence unequivocally characterized.

Table 3 ^{1}H NMR data for compounds 5 and 5a (600 MHz, δ in ppm and *J* in Hz)

No.	5[a,f]	5a[a]	5a[b]
1	6.96, d (9.8)	6.97, d (9.8)	6.92, d (9.8)
2	6.19, d (9.8)	6.19, d (9.8)	6.11, d (9.8)
6*α*	3.00, ddd (13.4, 3.5, 1.9)	2.95, ddd (13.4, 3.5, 1.8)	2.79, ddd (13.4, 3.6, 1.7)
6*β*	2.17, ddd (13.4, 12.8, 1.3)	2.16, ddd (13.4, 12.8, 1.3)	2.05, ddd (13.4, 12.8, 1.3)
7	1.62, tt (12.7, 3.6)	1.58, tt (12.5, 3.8)	1.43, tt (12.5, 3.8)
8*α*	1.83, m	1.80, m	1.68, m
8*β*	1.75, qd (13.1, 3.8)	1.75, qd (13.1, 3.9)	1.62, m
9*α*	1.27[c], m	1.26[d], m	1.11, td (13.1, 4.8)
9*β*	1.96, m	1.97, dt (13.2, 3.3)	1.89, dt (13.0, 3.2)
12	3.59, d (10.1)	3.49, d (11.0)	3.27, dd (10.8, 3.7)
	3.91, d (10.1)	3.53, d (11.0)	3.34[e], m
13	1.26, s	1.22, s	1.08, s
14	1.27[c], s	1.26[d], s	1.18, br s
15	1.91, br s	1.90, br s	1.79, s
11-OH			4.18, s
12-OH			4.54, br s

[a]Measured in methanol-d_4; [b]Measured in DMSO-d_6; [c,d]Overlapping signals; [e]Signals overlapped by solvent peak; [f]Data for sugar moiety: δ_H 4.30 (d, *J* = 7.8, H-1′), 3.88 (dd, *J* = 11.8, 2.0, H-6′a), 3.65 (dd, *J* = 11.8, 5.5, H-6′b), 3.36 (m, H-3′), 3.30 (m, H-4′), 3.27 (m, H-5′)

Apart from the aforementioned five new compounds, a known eudesmane sesquiterpenoid (**6**) was also separated and identified to be (1*R*, 7*R*, 10*R*, 11*R*)-12-hydroxyl anhuienosol that had been reported from *Silybum marianum* as a significant NO suppressant in BV-2 cells [13]. In addition, five chlorogenic acid analogues, namely, isochlorogenic acid A (**7**) [14], isochlorogenic acid A methyl ester (**8**) [15], methyl chlorogenate (**9**) [16], neochlorogenic acid methyl ester (**10**) [17] and cryptochlorogenic acid methyl ester (**11**) [18] (Fig. S1, Supporting Information), were also obtained in the present work, and they were identified on the basis of spectroscopic analyses and comparison with reported data in the literature.

Compounds **1**–**11** were tested in an *in vitro* anti-inflammatory assay by evaluating their inhibitory capability against LPS-induced NO production in RAW264.7 cells. While all other compounds showed only weak to no inhibition against NO release or displayed some cytotoxicity in the screening concentration range (Fig. S3, Supporting Information), the known isochlorogenic acid A (**7**) exerted a much better inhibitory effect (Fig. 6). The antihyperglycemic potential of all

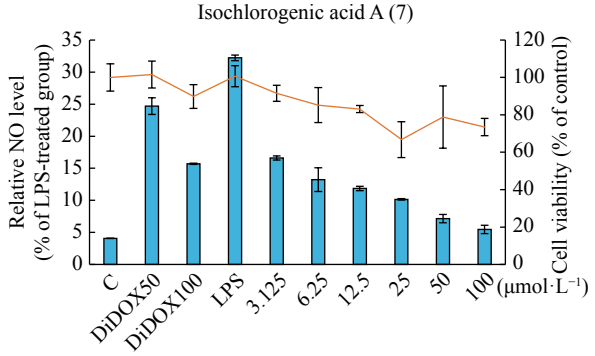

Fig. 6 Inhibitory effect of isochlorogenic acid A (7) on NO production in RAW 264.7 cells. Cells were treated with indicated concentrations of tested compounds along with LPS (1 μg·mL^{-1}) for 24 h, and then the accumulation of nitrite from the supernatants was evaluated by Griess reagent. Didox was used as a positive control. Column: relative NO level; Line: cell viability; C: Blank control

the isolates was also assessed *in vitro* by testing their *α*-glucosidase inhibitory activity, but unfortunately, none of them exhibited significant activity (< 50% inhibition) at the initial testing concentration of 80 μmol·L^{-1}.

Experimental

General experimental procedures

Optical rotations were measured on a Rudolph VI polarimeter (Rudolph Research Analytical, Hackettstown, NJ, USA) with a 10 cm length cell. ECD and UV spectra were recorded on a Chirascan Spectrometer (Applied Photophysics Ltd., Leatherhead, UK) with a 0.1 cm pathway cell. NMR experiments were conducted on a Bruker Avance DRX600 spectrometer (Bruker BioSpin AG, Fallanden, Switzerland) and referenced to residual solvent peaks (methanol-d_4: δ_H 3.31, δ_C 49.00; pyridine-d_5: δ_H 8.74, δ_C 150.35; DMSO-d_6: δ_H 2.50, δ_C 39.52). ESIMS analyses were carried out on an Agilent 1260-6460 Triple Quad LC-MS instrument (Agilent Technologies Inc., Waldbronn, Germany). HR-ESIMS spectra were obtained on an Agilent 6545 Q-TOF mass spectrometer (Agilent Technologies Inc., Waldbronn, Germany). X-ray crystallographic analysis was performed on Gemini E X-ray single crystal diffractometer (Agilent Technologies Inc., Waldbronn, Germany). HPLC separations were performed on an Agilent 1260 series LC instrument (Agilent Technologies Inc., Waldbronn, Germany) coupled with a YMC-Pack ODS-A column (5 μm, 10 mm × 250 mm, YMC Co., Ltd., Tokyo, Japan) at an elution rate of 3.0 mL·min^{-1} unless otherwise specified. Chiral HPLC analyses were carried out using a Chiral MZ(2)-RH (4.6 mm × 250 mm) column (Phenomenex, Washington D.C., USA). Column chromatography (CC) was performed on D101-macroporous absorption resin (Sinopharm Chemical Reagent Co., Ltd., Shanghai, China), MCI gel (CHP20P, Mitsubishi Chemical Corporation, Tokyo, Japan), reversed phase (RP) C_{18} silica gel (Merck KGaA, Darmstadt, Germany), Sephadex LH-20 (GE Healthcare Bio-Sciences AB, Uppsala, Sweden) and silica gel (300−400 mesh, Qingdao Marine Chemical Co., Ltd., Qingdao, China). All solvents used for CC were of analytical grade (Tianjin Fuyu Fine Chemical Co., Ltd., Tianjin, China) and solvents used for HPLC were of HPLC grade (Oceanpak Alexative Chemical Ltd., Goteborg, Sweden). Pre-coated silica gel GF_{254} plates (Qingdao Haiyang Chemical Co., Ltd., Qingdao, China) were used for thin-layer chromatography (TLC) monitoring.

Plant material

The flower buds of *Tussilago farfara* L. were collected in Dec. 2016 in Xiangyang, Hubei Province, China) and were authenticated by Prof. YE Guo-Hua from Shandong College of Traditional Chinese Medicine. A voucher specimen has been deposited at School of Biological Science and Technology, University of Jinan (Accession number: npmc-004).

Extraction and isolation

The dried flower buds of *T. farfara* (30 kg) were extracted with 95% EtOH at room temperature (3 × 7 days) to afford a crude extract (3.0 kg). The extract was suspended in 3.5 L water and partitioned successively with EtOAc (4 × 4.0 L) and *n*-BuOH (4 × 4.0 L) to afford the corresponding organic layers. The *n*-BuOH partition was dried *in vacuum* (531 g) and then subject to CC over D101-macroporous absorption resin (EtOH-H_2O, 30%, 50% and 95%) to afford three fractions (A, B and C). Fraction A (106.3 g) was fractionated on silica gel CC (EtOAc−MeOH−H_2O, 30 : 1 : 0.1 to 2 : 1 : 0.1) to produce four elutions (A1–A4). The elution A1 (4.9 g) was first separated by Sephadex LH-20 CC (in MeOH) to give four subfractions (A1-1–A1-4), and A1-1 was then chromatographed on an RP-C_{18} silica gel CC (MeOH-H_2O, 10% to 30%) to give another four subfractions (A1-1-1–A1-1-4). The subfraction A1-1-3 was fractionated by HPLC (30% MeCN−H_2O, respectively) to afford **1** (10.6 mg, t_R = 24.0 min) and **2** (9.8 mg, t_R = 25.1 min), while A1-1-4 yielded compound **6** (2.5 mg, t_R = 34.1 min) also by HPLC purification (35% MeCN−H_2O). Subfraction A1-2 (1.7 g) was separated by silica gel CC (CH_2Cl_2−MeOH-H_2O, 15 : 1 : 0.1 to 5 : 1 : 0.1) to produce another four subfractions (A1-2-1–A1-2-4), among which A1-2-3 was first processed with Sephadex LH-20 CC (in MeOH) and then purified by HPLC (30% MeCN−H_2O) to furnish **4** (1.0 mg, t_R = 17.0 min). Subfraction A2-2-4 was fractionated by HPLC (28% MeCN−H_2O) to yield **9** (20.0 mg, t_R = 10.1 min), **10** (2.5 mg, t_R = 6.7 min) and **11** (16.2 mg, $-t_R$ = 8.6 min). Fraction A1-4 (410.0 mg) was chromatographed on an RP-C_{18} silica gel CC (MeOH−H_2O, 10% to 30%) to give three subfractions (A1-4-1−A1-4-3), and then A1-4-1 was purified by HPLC (30% MeCN−H_2O) to yield **7** (9.8 mg, t_R = 7.0 min). Fraction A2 (5.2 g) was subject to Sephadex LH-20 CC (in MeOH) to give four subfractions (A2-1–A2-4). Subfraction A2-2 was chromatographed on an RP-C_{18} silica gel CC (MeOH−H_2O, 10% to 35%) to return three subfractions (A2-2-1–A2-2-3), and subfraction A2-2-2 was then separated by silica gel CC (CH_2Cl_2−MeOH−H_2O, 15 : 1 : 0.1 to 5 : 1 : 0.1) to give three further subfractions (A2-2-2-1–A2-2-2-3). Subfraction A2-2-

2-2waspurifiedbyHPLC(15%MeCN−H_2O)toafford**3**(1.4mg,t_R= 9.8 min). Fraction A2-3 was separated by an RP-C_{18} silica gel CC (MeOH−H_2O, 5% to 45%) to give four subfractions (A2-3-1−A2-3-4). Subfraction A2-3-4 was further purified by HPLC (28% MeCN−H_2O) to afford **8** (1.9 mg, t_R = 7.6 min). Fraction A4 (4.3 g) was first fractionated by Sephadex LH-20 CC (in MeOH) to give three subfractions (A4-1–A4-3), and A4-2 (1.5 g) was subject to silica gel CC (EtOAc-MeOH-H_2O, 30 : 1 : 0.1 to 10 : 1 : 0.1) to give two major subfractions (A4-2-1–A4-2-2), and A4-2-2 was further purified by HPLC (18% MeCN−H_2O) to afford **5** (10.0 mg, t_R = 11.9 min).

Identification of new compounds

Compound **1**: Colorless gum; $[\alpha]_D^{27}$ +327.6 (*c* 0.51, MeOH); UV (MeOH) λ_{max} (log ε) 298 (3.98); ECD (*c* 0.06, MeOH) λ_{max} ($\Delta\varepsilon$) 295 (+9.3) nm; ^{1}H and ^{13}C NMR data in methanol-d_4 see Tables 1 and 2; (+)-HR-ESIMS *m/z* 267.1593 $[M + H]^+$ (Calcd. for $C_{15}H_{23}O_4$, 267.1591).

Compound **2**: Colorless gum; $[\alpha]_D^{27}$ +275.0 (*c* 0.47, MeOH); UV (MeOH) λ_{max} (log ε) 298 (3.70); ECD (*c* 0.05, MeOH) λ_{max} ($\Delta\varepsilon$) 297 (+6.0) nm. ^{1}H and ^{13}C NMR data in methanol-d_4 see Tables 1 and 2; (+)-HR-ESIMS *m/z* 267.1593 $[M + H]^+$ (Calcd. for $C_{15}H_{23}O_4$, 267.1591).

Compound **3**: Colorless gum; $[\alpha]_D^{27}$ +120.2 (*c* 0.10, MeOH); UV (MeOH) λ_{max} (log ε) 295 (4.02); ECD (*c* 0.06, MeOH) λ_{max} ($\Delta\varepsilon$) 291 (+7.6), 345 (+2.4) nm. ^{1}H and ^{13}C NMR data in methanol-d_4 see Tables 1 and 2; (+)-HR-ESIMS *m/z* 283.1538 $[M + H]^+$ (Calcd. for $C_{15}H_{23}O_5$, 283.1540).

Compound **4**: Colorless gum; $[\alpha]_D^{27}$ −24.1 (*c* 0.10, MeOH); UV (MeOH) λ_{max} (log ε) 245 (4.02); ECD (*c* 0.08, MeOH) λ_{max} ($\Delta\varepsilon$) 204 (+5.9), 238 (+13.9), 268 (−2.0), 331 (−2.9) nm. ^{1}H and ^{13}C NMR data in methanol-d_4 and pyridine-d_5 see Tables 1 and 2; (+)-HR-ESIMS *m/z* 283.1537 $[M + H]^+$ (Calcd. for $C_{15}H_{23}O_5$, 283.1540).

Compound **5**: Colorless gum; $[\alpha]_D^{27}$ −56.6 (*c* 0.20, MeOH); UV (MeOH) λ_{max} (log ε) 239 (4.11); ECD (*c* 0.06, MeOH) λ_{max} ($\Delta\varepsilon$) 212 (+5.6), 264 (−17.6), 323 (−1.1) nm. ^{1}H and ^{13}C NMR data in methanol-d_4 see Tables 2 and 3; (+)-HR-ESIMS *m/z* 413.2165 $[M + H]^+$ (Calcd. for $C_{21}H_{33}O_8$, 413.2170).

*Enzymatic hydrolysis of **5** and absolute configuration determination of the sugar*

To a 2.0 mL buffer solution (NaOAc + HOAc, pH *ca.* 5.7) containing 6.0 mg compound **5** was added 6.0 mg snailase. The reaction mixture was kept at 37 °C in a water bath for 36 h and monitored by TLC. After the reaction, the aglycone was extracted with *n*-BuOH, and the water phase was dried and the acquired sugar was acetylated with excess acetic anhydride in 1.0 mL pyridine. The acetylation product and those prepared from standard $_D$ and $_L$ glucoses in the same way were then analyzed on a chiral MZ(2)-RH column. The *n*-BuOH partition was finally purified by HPLC (15% MeCN−H_2O) to afford the pure aglycone (**5a**, t_R = 10.0 min). Colorless gum; $[\alpha]_D^{27}$ −22.5 (*c* 0.10, MeOH); UV (MeOH) λ_{max} (log ε) 240 (4.01); ECD (*c* 0.06, MeOH) λ_{max} ($\Delta\varepsilon$) 214 (+3.9), 264 (−13.5), 329 (−1.4) nm. ^{1}H and ^{13}C NMR data in methanol-d_4 and DMSO-d_6 see Tables 2 and 3; (+)-HR-ESIMS *m/z* 251.1640 $[M + H]^+$ (Calcd. for $C_{15}H_{22}O_3$, 251.1642).

ECD calculations

The conformational analyses for the target isomers of compounds **1**, **4** and **5a** were performed by using the OPLS3 molecular mechanics force field *via* the Macro Model panel of Maestro 10.2. The conformers were further optimized with the software package Gaussian 09 at the B3LYP/6-311++G (2d,p) level, and the harmonic vibrational frequencies were also calculated to confirm their stability. The stable conformers were submitted to ECD calculation by time-dependent density functional theory (TD-DFT) method at the B3LYP/6-311++G (2d,p) level (solvent mode, MeOH). The ECD spectra of different conformers were simulated using a Gaussian function with a half-band width of 0.23 eV for all calculated compounds, and the final ECD spectra were obtained according to the Boltzmann distribution of each conformer. The calculated ECD spectra were then compared with the experimental ones.

*X-ray crystallographic analysis for **1***

$C_{15}H_{22}O_4$, M = 266.15, a = 9.4351(4) Å, b = 17.3241(7) Å, c =9.6734(5) Å, α = 90, β = 112.249(6), γ = 90, V = 1463.44(13) Å^3, T = 293(2) K, space group $P2_1$, Z = 2, μ (Cu Kα) = 0.747 mm^{-1}, 5257 reflections collected, 3837 independent reflections (R_{int} = 0.0173, R_{sigma} = 0.0290). The final R_1 value was 0.0354 ($I \geq 2\sigma$ (I)). The final wR_2 value was 0.0975 ($I \geq 2\sigma$ (I)). The final R_1 values were 0.0363 (all data). The final wR_2 value was 0.0988 (all data). The goodness-of-fit on F^2 was 1.038. Flack parameter = 0.19 (12).

The crystallographic data (excluding structure factor tables) for the reported structure (**1**) have been deposited at the Cambridge Crystallographic Data Center (CCDC) as supplementary publication (No. CCDC 2081028). Copies of the data can be obtained free of charge from the CCDC, 12 Union Road, Cambridge CB2 1EZ, UK (fax: Int. + 44(0) (1223) 336 033; e-mail: deposit@ccdc.cam.ac.uk). Details of the X-ray diffraction analysis data are described in the Supporting information (Table S5).

Bioassays

The NO production *inhibitory* assay was performed as we previously reported [18], and the α-glucosidase inhibitory assay was conducted according to a modified method in our recent work [9].

Supporting Information

Supporting information file contains the NMR and MS spectra for compounds **1**–**5** and **5a**, induced ECD spectra for **1**, **2**, **3** and **5a**, chiral HPLC analyses of sugar derivatives, structures of known chlorogenic acid analogues (**7**−**11**), NO inhibitory assays results for compounds **1**−**6** and **8**−**11**, re-optimized conformers, energies and proportions for isomers of compounds **1**, **4** and **5a**, and crystallographic data and structure refinement for **1**.

References

[1] Flora of China Editorial Committee of Chinese Academy of Sciences. *Flora of China* [M]. Beijing: Science Press, 1999: 93-94.

[2] Liu C, Wu H, Wang L, *et al*. Farfarae Flos: a review of botany, traditional uses, phytochemistry, pharmacology, and toxicology [J]. *J Ethnopharmacol*, 2020, **260**: 113038.

[3] National Pharmacopoeia Committee. *Pharmacopoeia of The People's Republic of China, Part 1* [M]. Beijing: China Medical Science and Technology Press, 2015: 332-333.

[4] Zhang JS, Cao XX, Yu JH, *et al*. Diarylheptanoids with NO production inhibitory activity from *Amomum kravanh* [J]. *Bioorg Med Chem Lett*, 2020, **30**(8): 127026.

[5] Yu SJ, Yu JH, Yu ZP, *et al*. Bioactive terpenoid constituents from *Eclipta prostrata* [J]. *Phytochemistry*, 2020, **170**: 112192.

[6] Yu JH, Yu ZP, Wang YY, *et al*. Triterpenoids and triterpenoid saponins from *Dipsacus asper* and their cytotoxic and antibacterial activities [J]. *Phytochemistry*, 2019, **162**: 241-249.

[7] Yu ZP, Yu JH, Zhang JS, *et al*. Inunicosides A−K, rare polyacylated ent-kaurane diterpenoid glycosides from the flowers of *Inula japonica* [J]. *Tetrahedron*, 2019, **75**(50): 130732.

[8] Yu SJ, Yu JH, He F, *et al*. New antibacterial thiophenes from *Eclipta prostrata* [J]. *Fitoterapia*, 2020, **142**: 104471.

[9] Sun J, Yu JH, Zhang JS, *et al*. Chromane enantiomers from the flower buds of *Tussilago farfara* L. and assignments of their absolute configurations [J]. *Chem Biodivers*, 2019, **16**(3): e1800581.

[10] Song XQ, Sun J, Yu JH, *et al*. Prenylated indole alkaloids and lignans from the flower buds of *Tussilago farfara* [J]. *Fitoterapia*, 2020, **146**: 104729.

[11] Song XQ, Yu JH, Sun J, *et al*. Bioactive sesquiterpenoids from the flower buds of *Tussilago farfara* [J]. *Bioorg Chem*, 2021, **107**: 104632.

[12] Bari LD, Pescitelli G, Pratelli C, *et al*. Determination of absolute configuration of acyclic 1,2-diols with $Mo_2(OAc)_4$. 1. Snatzke's method revisited [J]. *J Org Chem*, 2001, **66**(14): 4819-4825.

[13] Qin NB, Li SG, Yang XY, *et al*. Bioactive terpenoids from *Silybum marianum* and their suppression on NO release in LPS-induced BV-2 cells and interaction with iNOS [J]. *Bioorg Med Chem Lett*, 2017, **27**(10): 2161-2165.

[14] Zhu X, Zhang H, Lo R. Phenolic compounds from the leaf extract of artichoke (*Cynara scolymus* L.) and their antimicrobial activities [J]. *J Agric Food Chem*, 2004, **52**(24): 7272-7278.

[15] Lee EJ, Kim JS, Kim HP, *et al*. Phenolic constituents from the flower buds of *Lonicera japonica* and their 5-lipoxygenase inhibitory activities [J]. *Food Chem*, 2010, **120**(1): 134-139.

[16] Chen J, Mangelinckx S, Ma L, *et al*. Caffeoylquinic acid derivatives isolated from the aerial parts of *Gynura divaricata* and their yeast α-glucosidase and PTP1B inhibitory activity [J]. *Fitoterapia*, 2014, **99**: 1-6.

[17] Zhu X, Dong X, Wang Y, *et al*. Phenolic compounds from *Viburnum cylindricum* [J]. *Helv Chim Acta*, 2005, **88**(2): 339-342.

[18] Li YR, Li GH, Sun L, *et al*. Ingredients from *Litsea garrettii* as potential preventive agents against oxidative insult and inflammatory response [J]. *Oxid Med Cell Longev*, 2018, **2018**(23): 1-13.

Cite this article as: LI Yu-Peng, YANG Kang, MENG Hui, SHEN Tao, ZHANG Hua. Polyhydroxylated eudesmane sesquiterpenoids and sesquiterpenoid glucoside from the flower buds of *Tussilago farfara* [J]. *Chin J Nat Med*, 2022, **20**(4): 301-308.